Optical Engineering

OpticalEngineering.SPIEDigitalLibrary.org

Design and laser damage properties of a dichroic beam combiner coating for 22.5-deg incidence and S polarization with high transmission at 527 nm and high reflection at 1054 nm

John C. Bellum
Ella S. Field
Damon E. Kletecka
Patrick K. Rambo
Ian C. Smith

SPIE.

John C. Bellum, Ella S. Field, Damon E. Kletecka, Patrick K. Rambo, Ian C. Smith, "Design and laser damage properties of a dichroic beam combiner coating for 22.5-deg incidence and S polarization with high transmission at 527 nm and high reflection at 1054 nm," *Opt. Eng.* **56**(1), 011020 (2016), doi: 10.1117/1.OE.56.1.011020.

Design and laser damage properties of a dichroic beam combiner coating for 22.5-deg incidence and S polarization with high transmission at 527 nm and high reflection at 1054 nm

John C. Bellum,* Ella S. Field, Damon E. Kletecka, Patrick K. Rambo, and Ian C. Smith
Sandia National Laboratories, P.O. Box 5800, MS 1197, Albuquerque, New Mexico 87185, United States

Abstract. We designed a dichroic beam combiner coating with 11 HfO_2/SiO_2 layer pairs and deposited it on a large substrate. It provides high transmission (HT) at 527 nm and high reflection (HR) at 1054 nm for a 22.5-deg angle of incidence (AOI), S polarization (Spol), and uses near half-wave layer thicknesses for HT at 527 nm, modified for HR at 1054 nm. The two options for the beam combiner each require that a high intensity beam be incident on the coating from within the substrate (from glass). We analyze the laser-induced damage threshold (LIDT) differences between the two options in terms of the 527- and 1054-nm E-field behaviors for air → coating and glass → coating incidences. This indicates that LIDTs should be higher for air → coating than for glass → coating incidence. LIDT tests at the use AOI, Spol with ns pulses at 532 and 1064 nm confirm this, with glass → coating LIDTs about half that of air → coating LIDTs. These results clearly indicate that the best beam combiner option is for the high intensity 527 and 1054 nm beams to be incident on the coating from air and glass, respectively. [DOI: 10.1117/1.OE.56.1.011020]

Keywords: laser damage; dichroic optical coatings; laser beam combining coatings; coatings on large optics.

Paper 160636SSP received Apr. 27, 2016; accepted for publication Sep. 19, 2016; published online Oct. 12, 2016.

1 Introduction: the Dichroic Beam Combining Optic

This paper expands a conference proceedings paper[1] and also includes a correction to an error that we had not recognized in that paper or in the corresponding conference poster. The context of this work is that of Sandia's Z-Backlighter lasers[2] which produce kJ class, ns pulses of coherent light at 1054 nm. Frequency doubling of these pulses to 527 nm with an efficiency of ~70% is available in one of the beam trains. A beam-line configuration under development involves combining the high intensity, 527 nm, ns pulse beam with the high intensity, 1054 nm, ns pulse beam from a second Z-Backlighter beam train. The result will be two copropagating, kJ-class, ns-pulse beams with one at 527 nm and the other at 1054 nm. The 527 and 1054 nm copropagating pulses can overlap in time completely, partially, or not at all. Figure 1 shows this configuration's meter-class beam combining optic. It is a 61.5-cm diameter, 3.5-cm thick fused silica substrate providing a 22.5-deg angle of incidence (AOI) in air for both the 527- and 1054-nm high intensity beams which are in S polarization (Spol) and incident, respectively, from the left on side 1 and from the right on side 2 of the optic. The 1054-nm beam incident from the left in Fig. 1 has both Spol and Ppol components and is what remains after the ~70% efficient frequency doubling process, so is about one-third as intense as the 527-nm beam. The beam combining optic should simply reflect this residual 1054-nm beam, which will eventually terminate in a beam dump.

In the configuration of Fig. 1, a dichroic coating on the beam combining optic's side 1 would provide high transmission (HT) of the 527-nm beam and high reflection (HR) of the 1054-nm beam, while an antireflection (AR) coating on its side 2 would provide a high level of transmission for both beams. There could also be the opposite configuration, with the dichroic coating on side 2 and the 527-nm/1054-nm dual wavelength AR coating on side 1, and we will explore both of these options. In either option, the dichroic beam combiner coating, in addition to provide HT at 527 nm and HR at 1054 nm, needs to exhibit a high laser-induced damage threshold (LIDT) for both the 527- and 1054-nm, ns high intensity pulses. This requirement of high LIDT is especially challenging at 527 nm because those high intensity pulses, by virtue of the dichroic coating's HT at 527 nm, encounter each coating layer and layer interface at full intensity as they propagate through the coating.

2 Dichroic Beam Combiner Coating Design and Transmission/Reflection

Designing a dichroic coating that provides both HR at a laser's fundamental wavelength and HT at its second harmonic wavelength is challenging. A major design issue is dispersion in the refractive indices of the high and low index thin film layers. In our case, the differences due to dispersion are between the layer refractive indices at 527 and 1054 nm. For normal dispersion, which is characteristic of oxide dielectric layers, the index is greater at 527 nm than at 1054 nm, which means that layer thicknesses near that for

*Address all correspondence to: John Bellum, E-mail: jcbellu@sandia.gov

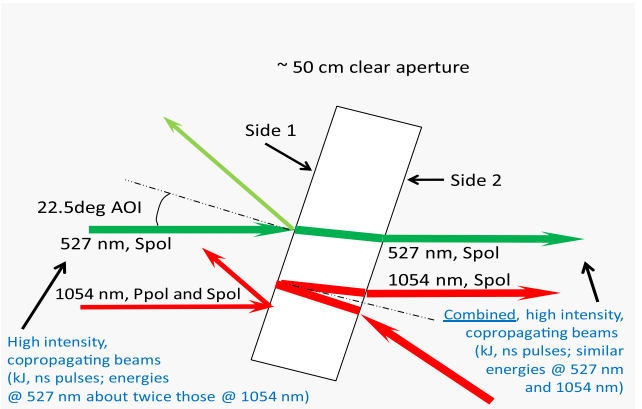

Fig. 1 Schematic illustration of the meter-class, dichroic beam combining optic and how it combines the high intensity, 527-nm beam incident from the left with the high intensity, 1054-nm beam incident from the right into the two high-intensity beams copropagating to the right.

the quarter-wave optical thickness (QWOT) required for HR at 1054 nm are thicker than layer thicknesses near that for the half-wave optical thickness (HWOT) required for HT at 527 nm. Because of this dispersion dilemma, there are two basic dichroic-coating design approaches. One approach is to start with a QWOT design for HR at a center wavelength of 1054 nm and based on the layer indices at 1054 nm, and then to alter layer thicknesses in a way that preserves HR at 1054 nm but also achieves HT at 527 nm. Another approach is to start with an HWOT design for HT at a center wavelength of 527 nm and based on the layer indices at 527 nm, and then to alter layer thicknesses in a way that preserves HT at 527 nm but also achieves HR at 1054 nm.

In the first approach, starting layers of thicknesses near that for QWOT at 1054 nm are thicker than for HWOT at 527 nm because the layer indices are less at 1054 nm than at 527 nm. In this case, the conditions of HWOT for these thicker layers, as constrained by dispersion, occur at lower layer indices and correspondingly higher wavelengths than 527 nm. In the second approach, starting layers of thicknesses near that for HWOT at 527 nm are thinner than layers for QWOT at 1054 nm because the layer indices are greater at 527 nm than at 1054 nm. Here, the conditions of QWOT for these thinner layers, as constrained by dispersion, occur at higher layer indices and correspondingly lower wavelengths than 1054 nm. The question is whether it is better to design around layers for QWOT and HR at 1054 nm in order to achieve near HWOT behaviors and HT at 527 nm, or to design around layers for HWOT and HT at 527 nm in order to achieve near QWOT behaviors and HR at 1054 nm.

Two factors favor designs centered about HT at 527 nm rather than HR at 1054 nm. First, the bandwidth for HT at the center wavelength of 527 nm is quite narrow compared to that for HR at the center wavelength of 1054 nm. This means that the design space for HT at 527 nm is smaller than that for HR at 1054 nm. Design space here refers to the range of layer thickness and refractive index combinations that support a particular transmission/reflection. Designs can stabilize HT with a 527-nm center wavelength within its narrow design space and then accommodate HR at 1054 nm based on modifications that overlap its large design space, or stabilize HR with 1054-nm center wavelength within its large design space and then accommodate HT at 527 nm based on modifications that overlap its narrow design space. The former design process stabilizes HT at 527 nm within its entire, although smaller, design space, but the latter design process achieves HT at 527 nm by using only a portion of its smaller design space as limited by stabilizing HR with the 1054-nm center wavelength. For these reasons, the stability of designs with respect to HT at 527 nm should be higher for the former design process than for the latter design process. On the other hand, both design processes have stable HR properties near 1054 nm because of the broad bandwidth and large design space for HR. The former design process involves HR center wavelengths that are shorter than 1054 nm. This is consistent with the above discussion. Such designs rely on the large bandwidths for acceptable HR to be broad enough to include 1054 nm. The latter design process involves HT center wavelengths that are larger than 527 nm, but the bandwidths for this HT are broad enough to include 527 nm only within a small portion of the already small available design space.

The second factor has to do with the sensitivity of a dichroic coating design to variations in layer thicknesses and indices of refraction associated with practical deposition processes.[3] Every design is based on the actual dispersion data of the high and low index thin film materials used in the deposition of the coating. Layer index and thickness variations, usually random and slight,[3] are likely to have the least effect on coating performance that is associated with layer thicknesses and refractive indices of the most stable coating designs within the design space. According to the above explanation, it is plausible that the most stable designs for both HT at 527 nm and HR at 1054 nm should be those that derive from the design space for HT at 527 nm, and those designs should be the least affected by deposition process variations. Likewise, the less stable designs should derive from the design space for HR at 1054 nm to achieve HT at 527 nm, and should be more vulnerable to deposition process variations. The HT performance at 527 nm of coatings based on such designs often exhibits a "half-wave" dip in transmission at 527 nm, which we have observed previously.[4] This may be due to process variations upsetting the delicate balance of the design layer thicknesses that led to HT at 527 nm within a design space that mostly favors HWOT and HT behaviors at wavelengths greater than 527 nm. In any case, the "half-wave" transmission dip is undesirable and its elimination is a focus of coating research.[5–8]

From the preceding discussion, design layers for near HWOT and stabile HT at a center wavelength of 527 nm will be layers for near QWOT and stable HR at center wavelengths less than 1054 nm, but broad HR bandwidth at these wavelengths offers the prospect that HR can still be good at 1054 nm. We followed this design approach using the OptiLayer Thin Film Software[9] to explore dichroic coatings consisting of HfO_2/SiO_2 layer pairs on a fused silica substrate and providing optimal HT at a center wavelength of 527 nm for 22.5-deg AOI and Spol, and at the same time affording good HR at 1054 nm for 22.5-deg AOI and both Spol and Ppol. This meant using lower center wavelengths for the HR band such that its high wavelength band edge remained high enough for the reflectivity at 1054 nm to still be high ($R_{Spol} \sim 99\%$ and $R_{Ppol} \sim 98.5\%$). For such HR center wavelengths that are less than 1054 nm, the "half wave" dip in transmission mentioned

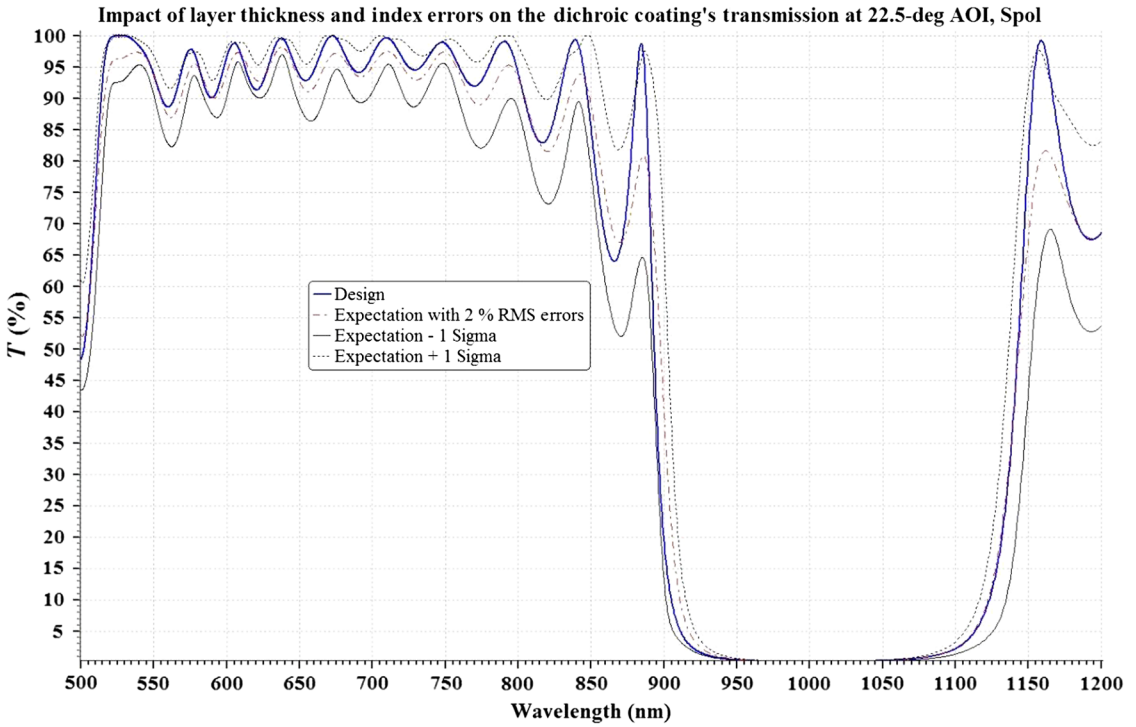

Fig. 2 Analysis of layer thickness and index errors on the transmission properties of the dichroic coating at 22.5-deg AOI, Spol. The legend delineates the design transmission, the expectation of what the transmission might be in the case of 2% RMS errors in layer thicknesses and refractive indices, and the range of transmission corresponding to a 1 sigma (1 standard deviation) extent of such errors.

above should occur at wavelengths that are less than 527 nm. A design goal was to use as few layers as possible, in order to favor higher LIDTs by virtue of a minimal number of layers and layer boundaries through which the high intensity 527 nm pulses would need to propagate. We found that 22 layers (11 HfO_2/SiO_2 layer pairs) were adequate for the design, which provides HT at 22.5-deg AOI, Spol of essentially 100% at 527 nm. That is for the coating alone on a fused silica substrate and does not include the Fresnel reflection of the uncoated side of the substrate. Figure 2 shows this together with results of an OptiLayer analysis of the impact on the design transmission spectrum that layer thickness and index errors can have at the 2% RMS level and within a 1 sigma (1 standard deviation) variation from that level. According to this analysis, random layer thickness and index errors that commonly occur during deposition processes can significantly compromise the HT at 527 nm, with expectations for it down from ~100% for the design to ~96.5% and ~93% in the case of 2% RMS errors and errors within 1 standard deviation from this, respectively. Even with these considerably lower levels of transmission, the coating's basic HT spectral feature at wavelengths in the vicinity of 527 nm remains evident despite such layer thickness and index errors. In addition, the layer errors have essentially no effect on the HR behavior at 1054 nm. So, we can reasonably expect dichroic coatings that we deposit using our design to exhibit this or a similar result.

We deposited the dichroic coating of our design in Sandia's large optics coater[10,11] by ion-assisted e-beam evaporation of SiO_2 for the SiO_2 layers, and of Hf in a reactive process using an oxygen back pressure for the HfO_2 layers. The first layer to be deposited on the fused silica substrate is HfO_2, and we refer to it as the innermost layer. The outermost layer is a SiO_2 layer of thickness near that of an HWOT at 1054 nm, and it interfaces with the incident medium, which is air. The coating exhibited an HT band with center wavelength near 527 nm, as confirmed by its transmission spectra from measurements with a PerkinElmer Lambda 950 Spectrophotometer. These spectra are shown in Figs. 3 and 4, which present both the design and measurement transmission spectra for our dichroic coating at 22.5-deg AOI and Spol and Ppol, respectively.

Unlike in Fig. 2, transmission shown in Figs. 3 and 4 is determined not only by the coating on a fused silica optic but also by losses due to Fresnel reflection on the other side of the optic. Accordingly, the design HT for Spol at 527 nm is ~96.6% in Fig. 3 corresponding to design Fresnel reflection losses for Spol of ~3.4%. For Ppol, this design HT is ~97.5% (Fig. 4) corresponding to design Fresnel reflection losses for Ppol of ~2.5%. These design Fresnel losses are specified in the OptiLayer application by generic dispersion properties of fused silica, and may deviate from the actual Fresnel losses of the crystalline fused quartz witness optic on which we deposited the coating. We must keep this in mind regarding the spectrophotometer measurements, which account for the actual Spol and Ppol Fresnel losses of the witness optic. These measurements show Ppol transmission of ~94% at 22.5-deg AOI (Fig. 4), slightly higher than its Spol counterpart of ~93.5% (Fig. 3). The similarity of these transmissions is not surprising considering the low, 22.5-deg AOI. The accuracy provided by the Lambda 950 spectrophotometer for these HT results is ±0.2%. If the

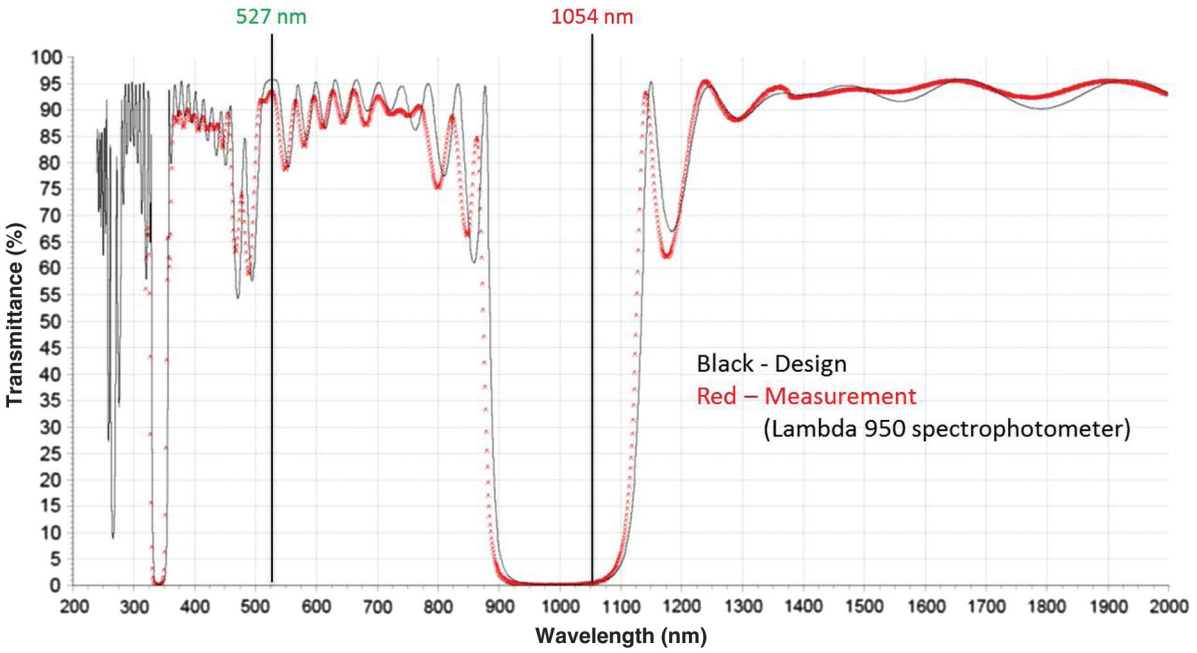

Fig. 3 Transmission according to design and measurement for the dichroic beam combiner coating for 22.5-deg AOI, Spol.

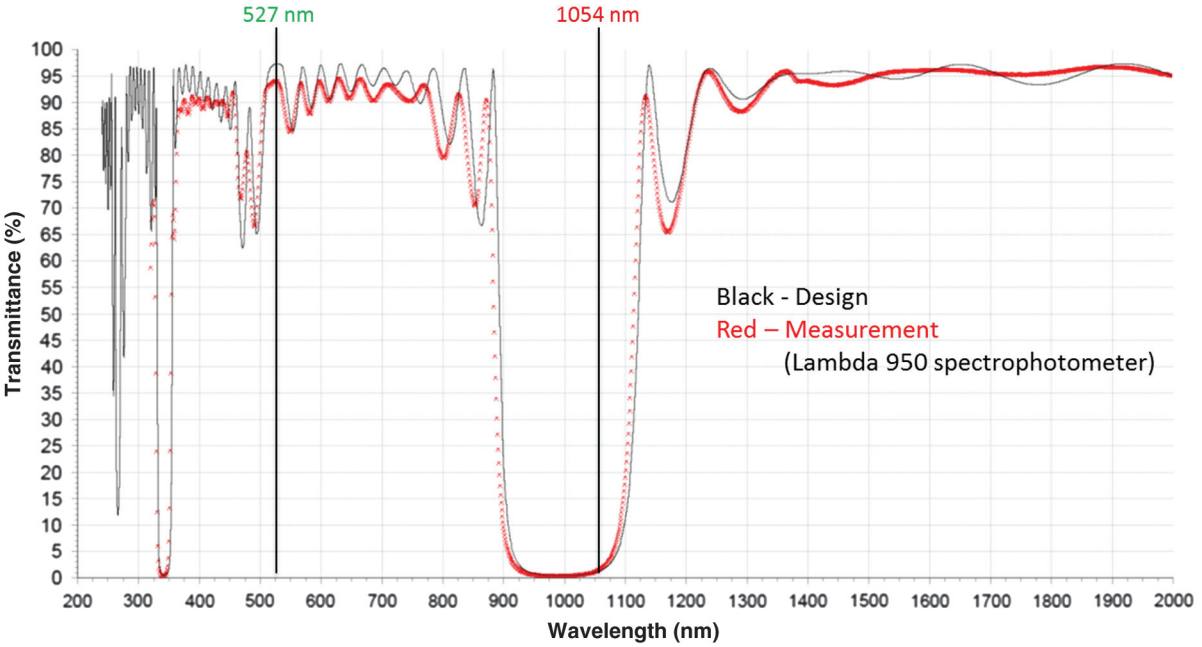

Fig. 4 Transmission according to design and measurement for the dichroic beam combiner coating for 22.5-deg AOI, Ppol.

actual and design Fresnel losses are the same, then these measurements would imply Spol and Ppol transmissions for just the coating of ~96.9% and ~96.5%, respectively. This result is reasonable, considering the measurement accuracy, even though we would expect the Ppol transmission to be higher than that for Spol. According to preliminary measurements using Sandia's large optics reflectometer, we estimated the reflectivities at 527 nm and 22.5-deg AOI for just the coating to be ~3.5% for Spol and ~3.2% for Ppol, which would indicate respective transmissions of ~96.5% and ~96.8%. This result, which provides a higher transmission for Ppol than for Spol, is also reasonable considering measurement accuracies. We are looking into more precise ways of measuring the transmission of the coating and verifying the Fresnel reflection of our fused silica witness optics in order to resolve these uncertainties.

The "half-wave" transmission dips of Figs. 3 and 4 occur at wavelengths between ~460 and ~500 nm, which are less than 527 nm and are consistent with what we mentioned earlier. Also, it is evident in Figs. 3 and 4 that the deposited

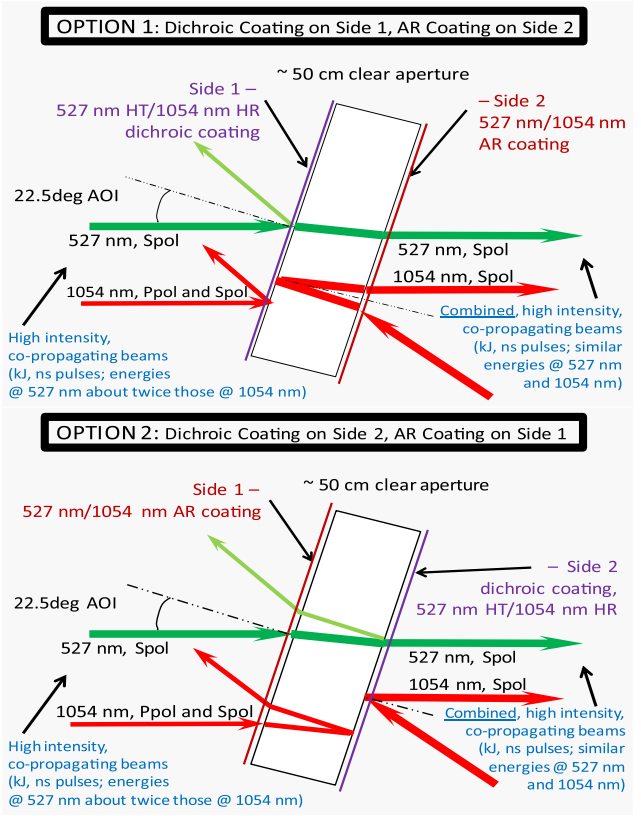

Fig. 5 Schematic illustrations of option 1 (top illustration) and option 2 (bottom illustration) for the dichroic beam combining optic.

coating's HT at 527 nm fails by ~3% to reach that of the coating design, which is ~96.6% with the design Fresnel reflection losses of ~3.4%. This is in keeping with the error analysis of Fig. 2. We have, in fact, deposited several dichroic coatings, and they have all exhibited HT bands with center wavelengths near 527 nm, in agreement with the spectra of Figs. 3 and 4 and the error analysis of Fig. 2. The specific shapes and widths of the HT bands did vary from coating run to coating run, and HT at 527 nm for the corresponding transmission spectra varied somewhat at values ~3% less than the design value. At the same time, the coatings' reflection at 1054 nm remained similar to that of the coating design. This indicates that the layer thickness and index variations of our deposition processes are probably in the range of 2% RMS or less. The level of transmission performance at 527 and 1054 nm, though not the best that it could be according to the design, is nevertheless adequate enough for the beam combining role of the dichroic coating.

3 Dichroic Beam Combining Options

Figure 5 shows the two options for the dichroic beam combining optic. For option 1, the dichroic beam combiner coating is on side 1 and a 527-nm/1054-nm AR coating is on side 2 of the beam combining optic, and vice versa for option 2. The main difference between these two options is that the high intensity, 527- and 1054-nm Spol pulses are incident on the dichroic coating from air and from within the substrate (from glass), respectively, in option 1, and from glass and from air, respectively, in option 2. We restrict our attention in this study to only the dichroic beam combining coating and to how it performs in the configurations of options 1 and 2. The 527-nm/1054-nm AR coating of Fig. 5 is the same as the side 2 AR coating of a 22.5-deg AOI diagnostic beamsplitter. A previous report[11] describes this coating's AR properties, with Spol and Ppol reflectivities for air → coating incidence at 22.5 deg of 0.37% and 0.24%, respectively, at 527 nm, and 1.15% and 0.6%, respectively, at 1054 nm. Another previous report[12] describes its design and E-field properties for air → coating incidence at 22.5 deg, and also its Spol and Ppol LIDTs of 11 and 13 J/cm^2, respectively, at 532 nm, and 46 and 55 J/cm^2, respectively, at 1064 nm.

4 Dichroic Coating E-Fields for Incidence from Air and from the Substrate

In optimizing HT at 527 nm and HR at 1054 nm using our design approach described above, we treat the light as being incident on the dichroic coating from air. Yet, either the 527-nm or the 1054-nm high intensity pulses must be incident on the dichroic coating from glass according to options 1 or 2 for the dichroic beam combining optic (see Fig. 5). The question is whether there are differences between options 1 and 2, and, if so, whether the differences matter. As to transmission and reflection properties of the coating, there are no differences between options 1 and 2. Conservation of energy for the propagation of light ensures this. Therefore, we decided to look for differences in the E-field behaviors at 527 and 1054 nm for incidence on the dichroic coating from air and from glass when the AOI in air is 22.5 deg.

It is common, from a deposition point of view, to think of a coating relative to its incident medium, with the innermost layer at the substrate/coating interface and the outermost layer at the incident medium/coating interface. Examining the E-fields for options 1 and 2 involves this conventional thinking as well as the reverse of this thinking. We identify the innermost and outermost layers in the conventional way. The dichroic beam combining optic is fused silica glass. For this substrate, the 22.5-deg AOI in air corresponds to 15.2-deg AOI in the glass. This AOI in glass is about the same for both 527 and 1054 nm owing to the very mild dispersion of fused silica.

We used the OptiLayer Thin Film Software[9] to calculate the standing-wave E-field intensities at 527 and 1054 nm for light incident on the dichroic beam combiner coating from air and from glass at an AOI in air of 22.5 deg. Figures 6 and 7 show these E-field intensities, for both Spol and Ppol, at 527 and 1054 nm, respectively. It was at this point in our preparation of the conference poster presentation and proceedings paper[1] that the error we mentioned in Sec. 1 occurred. At that time, our OptiLayer calculations of E-field intensities were correct for air → coating incidence, but we mistakenly used incorrect parameters in the E-field intensity calculations for glass → coating incidence. We have remedied that error, and Figs. 6 and 7, unlike their counterparts in our proceedings paper,[1] present correct E-field intensities, not only for air → coating incidence but also for glass → coating incidence. We have expanded and somewhat altered the analysis and discussion of this paper in comparison to our proceedings paper in order to account for these correct E-field behaviors.

The E-field intensities of Figs. 6 and 7 refer to $|\mathbf{E}|^2$, where $\mathbf{E}$ is the E-field amplitude, and the $|\mathbf{E}|^2$ values are in percent relative to a normalized value of 100% for the incident

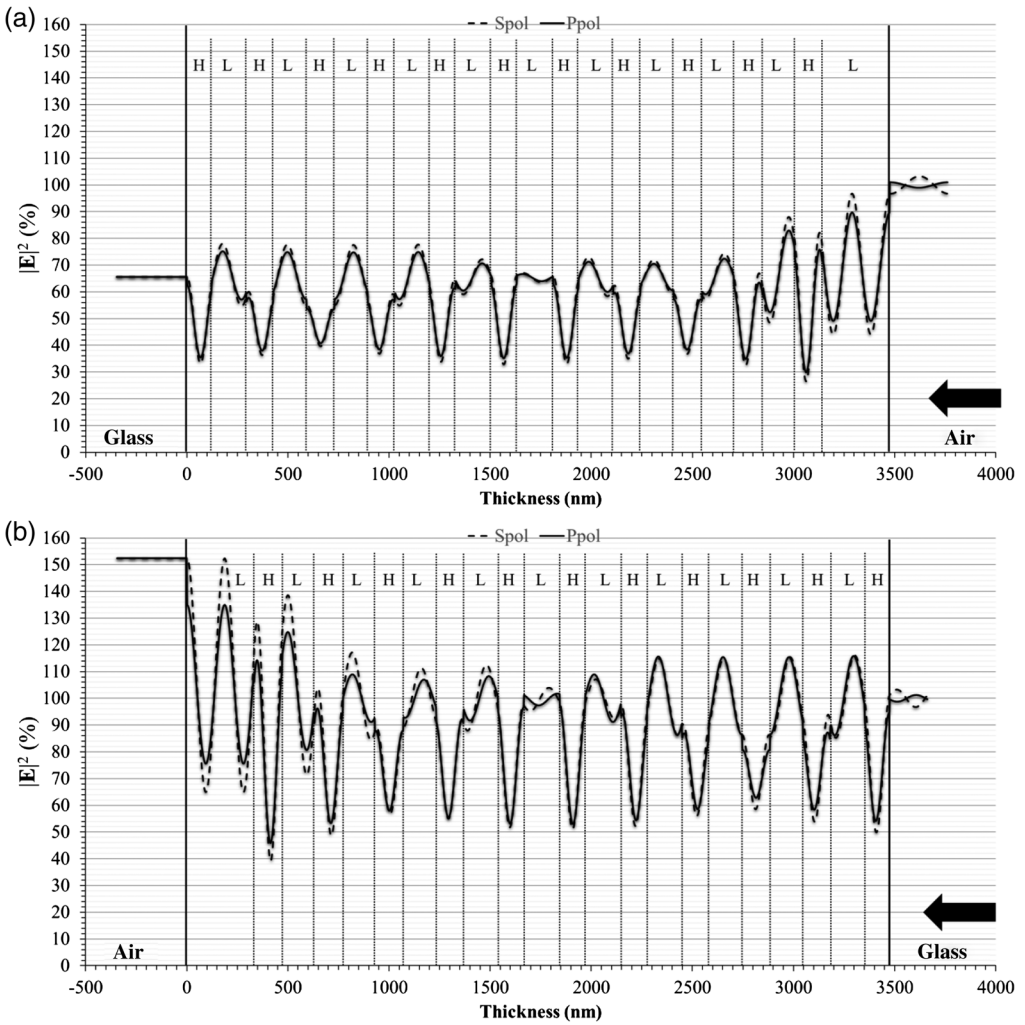

Fig. 6 Design E-field intensities, $|\mathbf{E}|^2$ (see text), as a percent of incident intensity at 527 nm for incidence on the dichroic beam combiner coating from (a) air and from (b) glass at 22.5-deg AOI in air and Spol and Ppol as indicated. The arrows indicate the direction of incidence. The left-hand and right-hand vertical lines mark the air-coating and glass-coating interface locations, respectively, the other vertical lines mark the layer interface locations, and L and H designate, SiO_2 and HfO_2 layers, respectively.

E-field intensity. The normalized incident intensity is in air at the air-coating interface for air → coating incidence, and in glass at the substrate-coating interface for glass → coating incidence. At 527 nm (Fig. 6), the intensities oscillate layer-to-layer through the coating at strengths ranging from moderately low to high, in keeping with the HT of the design. At 1054 nm (Fig. 7), the intensities strongly peak in the incident medium and quench rapidly into the coating layers, in keeping with the HR of the design. In all cases, the Spol and Ppol E-fields are similar to each other, consistent with the relatively small 22.5-deg AOI in air. There are, however, significant differences for both 527 and 1054 nm between the air → coating and glass → coating E-field behaviors.

In the case of 527 nm and air → coating incidence [Fig. 6(a)], all major E-field intensity peaks except two Spol peaks and two Ppol peaks occur in the higher band gap SiO_2 layers while E-field intensity minima, in the range of 30% to 40% of the incident intensity, occur in the lower band gap HfO_2 layers. Also, most of the major E-field intensity peaks are of moderate strength, in the range of 70% to 80% of the incident intensity. Such E-field behavior is favorable to high LIDTs. The strongest Spol and Ppol intensity peaks, at 75% to 95% of incident intensity, occur in the three outermost (in the conventional sense) layers, and include two of the exceptions we just mentioned, an Spol peak and a Ppol peak that are in the outermost HfO_2 layer. This latter E-field behavior is less favorable to high LIDTs because of the higher E-field intensities, especially in the lower band gap HfO_2 layer.

For glass → coating incidence at 527 nm [Fig. 6(b)], the overall E-field behaviors are not favorable to higher LIDTs. Even though all E-field intensity peaks except two Spol peaks and two Ppol peaks occur in higher band gap SiO_2 layers, and most E-field intensity minima occur in lower band gap HfO_2 layers, the intensity peaks and minima in this case are at higher levels, in the ranges of 110% to 150% for peaks and 50% to 60% for minima. The outermost and next-to-outermost HfO_2 layers are the ones with Spol and Ppol intensity peaks, at levels of ~114% to 128% and ~95% to 102%, respectively [Fig. 6(b)]. These peak intensities are higher than their ~75% to 80% and ~64% to 67%

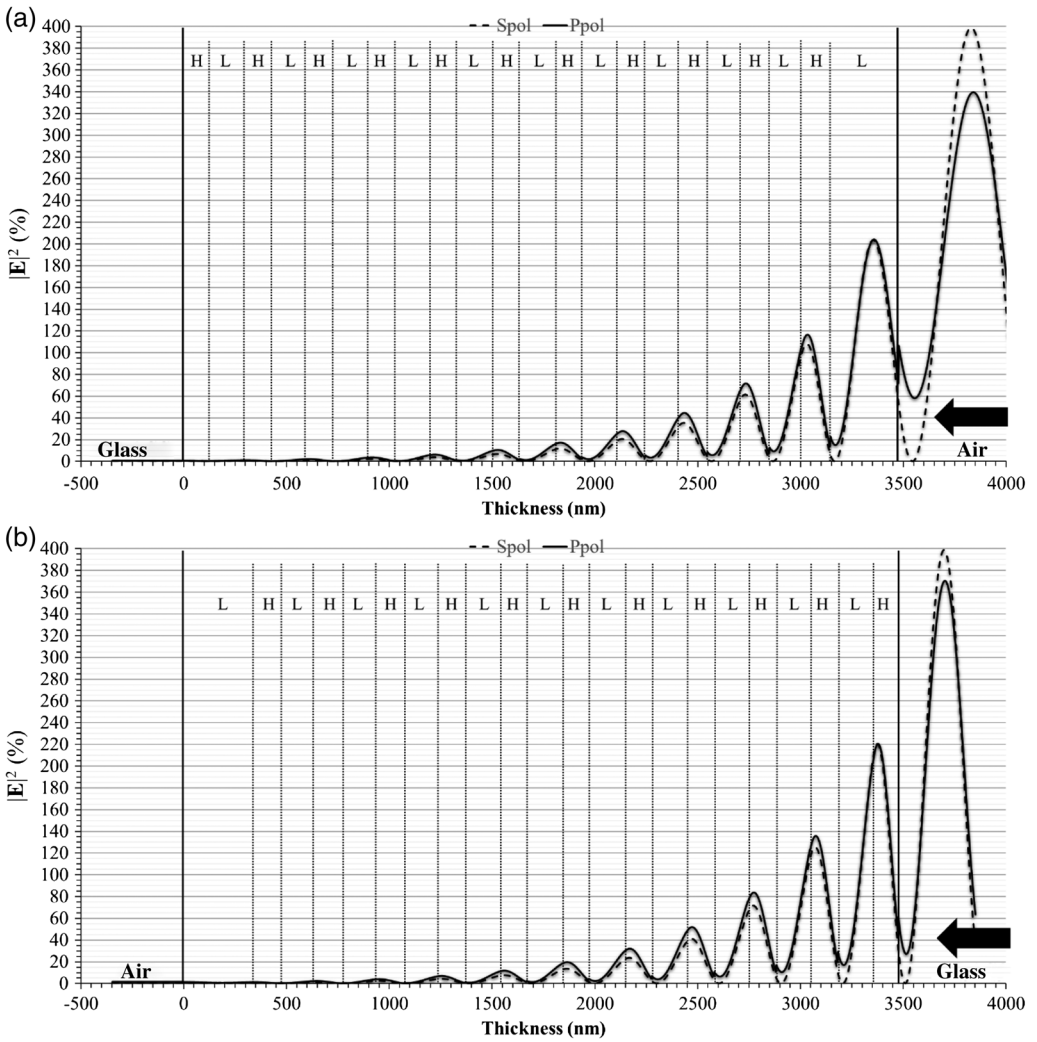

Fig. 7 Design E-field intensities, $|\mathbf{E}|^2$ (see text), as a percent of incident intensity at 1054 nm for incidence on the dichroic beam combiner coating from (a) air and from (b) glass at 22.5-deg AOI in air and Spol and Ppol as indicated. The arrows indicate the direction of incidence. The left-hand and right-hand vertical lines mark the air-coating and glass-coating interface locations, respectively, the other vertical lines mark the layer interface locations, and L and H designate SiO_2 and HfO_2 layers, respectively.

counterparts in the two outermost HfO_2 layers for air → coating incidence [Fig. 6(a)]. Intensity peaks in HfO_2 layers, due to their low band gap, can enhance intrinsic laser damage, especially at 527 nm for which the photon energy is higher compared to 1054 nm. Extrinsic laser damage may also occur for 527 nm, particularly at locations where intensity and extrinsic defect levels are high. The higher peak and minimum intensities throughout the coating for glass → coating incidence in comparison to air → coating incidence indicate that the occurrence of extrinsic laser damage is more probable in the former case. These factors make glass → coating incidence at 527 nm less favorable to high LIDTs overall than air → coating incidence.

The differences between the E-fields for air → coating and glass → coating incidence for 1054 nm also indicate that the former favors higher LIDTs than the latter. In the air → coating case [Fig. 7(a)], the highest E-field intensity peak, at ~200% of incident intensity for both Spol and Ppol, occurs within the outermost SiO_2 layer. Though this peak intensity is quite high, its laser damage effects are mitigated by the higher band gap of SiO_2. The next highest intensity peaks, at ~110% to 120% of incident intensity, occur in the outermost HfO_2 layer near its interface with the next to outermost SiO_2 layer. For reasons explained above, this is not favorable to a high LIDT. However, all other E-field intensity peaks quench rapidly into the coating. In addition, the major Spol and Ppol intensity peaks, at ~350% to ~400% of incident intensity, occur in air, which affords very high resistance to optical E-field breakdown. Overall, these E-field behaviors are at least moderately favorable to high LIDTs.

In the glass → coating case [Fig. 7(b)], the highest peak E-field intensities in the coating are ~220% of incident intensity for both Spol and Ppol and occur in the innermost HfO_2 layer near its interface with the first SiO_2 layer. These intensity peaks are twice as strong as their counterparts for air → coating incidence, making them very unfavorable to high LIDTs. In addition, major Spol and Ppol E-field intensity peaks, at ~350% to 400% of incident intensity, occur in the glass substrate at a depth of about 300 nm, which is within the optically polished substrate surface's Beilby layer where we[13] and others[14–16] have found evidence of

trace levels of polishing compound contamination within the substrate microstructure that can be responsible for laser-induced damage occurring at lower threshold fluences. This means that these major intensity peaks in the incident medium associated with HR will limit LIDT for glass → coating incidence much more effectively than for air → coating incidence.

We can sum up our findings as follows. Air → coating incidence and glass → coating incidence are equivalent with respect to any coating's transmission and reflection, which is well known. They are, however, not equivalent with respect to E-field behaviors. These E-field differences for our dichroic beam combiner coating indicate that air → coating incidence is overall more favorable to high LIDTs than glass → coating incidence for both HT at 527 nm and HR at 1054 nm.

5 Dichroic Coating LIDTs for Incidence from Air and from the Substrate

To check the validity of our E-field analysis and determine its actual laser damage implications, we had LIDT tests performed on our dichroic coating by Spica Technologies, Inc.[17] The LIDT tests were conducted according to the NIF-MEL protocol[18] with 3.5-ns pulses at both 532 and 1064 nm and for incidence on the coating from glass and from air at 22.5-deg AOI in air and Spol. OptiLayer Thin Film Software[9] calculations confirm that E-field intensity peaks under these conditions at 532 and 1064 nm for our dichroic coating design do not shift in location within the coating compared to their counterparts at 527 and 1054 nm. The peak intensities within the coating can, however, increase or decrease slightly (within less than ~5%) in strength. We are mindful of these intensity differences when analyzing LIDT results for 532 and 1064 nm in terms of the E-field behaviors at 527 and 1054 nm. The dichroic coating was on one side of a 50-mm diameter, 10-mm thick fused silica substrate that underwent optical polishing on both sides. The other side of the optic was uncoated. For incidence on the coating from glass, the laser pulses were incident on the uncoated side of the optic and propagated through the fused silica substrate to the coated side. Laser damage occurred exclusively on the coated side of the optic in all cases.

For context, we repeat a description of the NIF-MEL protocol[18] as it applies to the LIDT tests of this study. The 3.5-ns pulses are multilongitudinal mode with a Gaussian (TEM_{00}) transverse beam profile having a $1/e^2$ diameter of ~1 mm. The pulse repetition rate is 5 Hz, and there is a sequence of raster scans of the laser beam spot over the same dense set of ~2500 sites covering a 1 cm × 1 cm area of the coating. Each scan is at a single fluence starting with a low fluence with successive scans at increasingly higher fluences. The scan rate is such that each raster scan site receives one laser pulse at each fluence level. The beam spots at adjacent scan sites overlap each other at 90% of their peak intensities. Because of this strong site-to-site overlap of the beam spots, a pulse incident at one site exposes the previous and neighboring scan sites to significant fluence levels that may influence laser damage at those nearby sites. A camera detects damage, site-by-site, both nonpropagating (NP) damage, which occurs but does not grow due to subsequent pulses in the raster scan or to pulses at higher fluence in a subsequent scan, as well as propagating damage,

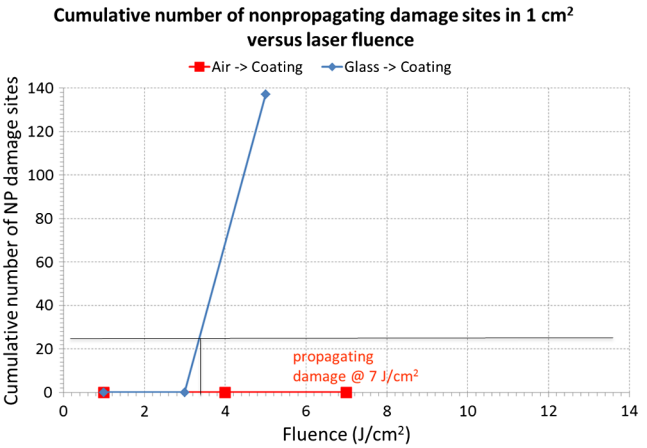

Fig. 8 Laser damage data for the dichroic beam combiner coating at 532 nm and 22.5-deg AOI in air, Spol, and incidence on the coating from air (air → coating) and from glass (glass → coating). Lines connecting the data points are guides for the eye. The $1/e^2$ transverse beam diameters were 1.06 mm and 1.03 mm for the air → coating and glass → coating LIDT tests, respectively. See text for explanation of NP and propagating damage.

which occurs and continues to grow due either to subsequent pulses in the raster scan or to pulses at higher fluence in a subsequent scan. LIDT is determined either by the fluence at which the accumulated number of NP damage sites exceeds 25 (i.e., ~1% of the total number of raster scan sites), or by the fluence at which propagating damage occurs at one or more sites, whichever is the lower fluence.

For further context, we summarize important aspects of extrinsic and intrinsic laser damage mechanisms, both of which we can expect to be at play to varying degrees for our laser wavelengths and ns laser pulses. Extrinsic mechanisms primarily depend on material heating processes that take place on ns time scales due to absorption of laser energy by foreign, microstructural defects such as contaminants, particulates, or nodules within the coating or beneath the optically polished substrate surface.[19–22] Such mechanisms can lead to NP as well as propagating damage. On the other hand, intrinsic mechanisms primarily depend on direct laser excitation of electronic transitions to conduction bands of the coating molecules.[22,23] As such, these intrinsic mechanisms are governed more by the coating materials themselves and their electronic properties, including electronic defect states that lie between the valence and conduction bands and can be more prevalent in the vicinity of nanoscale structural defects within the coating. Intrinsic mechanisms usually lead to propagating damage and, because they depend on laser excitation of electronic transitions, are more effectively driven by pulses of higher photon energy (in our case, the pulses at 527 or 532 nm) than those of lower photon energy (in our case, the pulses at 1054 or 1064 nm).

Figure 8 shows the results of the Spol LIDT tests at 532 nm in terms of cumulative number of NP damage sites as a function of laser fluence. There are sharp contrasts in the LIDT behaviors between air → coating incidence and glass → coating incidence. In the case of air → coating incidence, there is no NP damage at all and the LIDT is due to propagating damage occurring at 7 J/cm^2. In the case of glass → coating incidence, the LIDT is due to precipitous accumulation of NP damage, from none at 3 J/cm^2 to 134 NP damage sites at 5 J/cm^2. These latter two data points

are insufficient to describe how this sharp increase in NP damage actually depends on fluence levels between 3 and 5 J/cm^2. In particular, we do not exactly know the threshold fluence at which 25 NP damage sites would have occurred. The line that serves as a guide for the eye between the two points provides a linear interpolation (shown by the short, black vertical line in Fig. 8) of 3.4 J/cm^2 for the threshold fluence, but that result is not reliable. All that we can say from the data of Fig. 8 is that the LIDT for glass → coating incidence is in the range of (4 ± 1) J/cm^2 (i.e., between 3 and 5 J/cm^2) and is due to a sharp increase in NP damage. This LIDT is less than the 7 J/cm^2 LIDT for air → coating incidence by a factor of 0.57 ± 0.14.

The Spol LIDT behaviors at 532 nm (Fig. 8) correlate well with our analysis above of the corresponding air → coating and glass → coating E-field intensities of Fig. 6 for 527 nm. For the air → coating case [Fig. 6(a)], two of the major intensity peaks occur in HfO_2 layers, namely, the peaks at levels of ~82% and ~67% in the outermost and next-to-outermost HfO_2 layers, respectively. All other major intensity peaks are in higher band gap SiO_2 layers. We expect that the outermost HfO_2 layer is the most likely place for laser damage to occur for air → coating incidence at 532 or 527 nm, and that the damage is intrinsic to HfO_2, consistent with the catastrophic, propagating laser damage at a threshold of 7 J/cm^2 (Fig. 8).

In the glass → coating case, the question is why abrupt accumulation of NP damage occurs for 532 nm at fluences well below the 7 J/cm^2 threshold for intrinsic, propagating damage in the case of incidence from air. Such NP damage behavior would be explained by high E-field intensities at locations of high density of extrinsic defects such as contamination, particulates, or nodules. The locations for the highest densities of extrinsic defects are most likely within the first few coating layers next to the polished substrate surface[21,22] and within its Beilby layer.[14–16] As is evident for glass → coating incidence at 527 nm in Spol [Fig. 6(b)], the E-field intensities within the Beilby layer are fairly level and close to 100% of incident intensity. These intensities may be high enough to initiate NP damage mediated by extrinsic, polishing compound contamination within the Beilby layer. In addition, conditions are favorable to NP damage occurring within the innermost layers because they tend to have higher density of extrinsic, particulate, or nodule defects,[21,22] and they experience fairly high E-field intensities at 527 nm for incidence from glass [Fig. 6(b)], with minima at ~50% to 60% levels for the HfO_2 layers and peaks at a level of ~115% for the SiO_2 layers. These intensity levels are significantly higher than their counterparts for air → coating incidence, where the minima in the inner HfO_2 layers are at ~35% to 40% levels and the peaks in the inner SiO_2 layers are ~75% [Fig. 6(a)]. As such, they can more effectively lead to NP damage governed by extrinsic defects (particulates or nodules) that are usually more prevalent in the initial coating layers next to the substrate.[21,22]

We believe these intensity behaviors at prime locations for extrinsic defects correlate well with and adequately explain the sharp onset of NP damage at fluences between 3 and 5 J/cm^2 (Fig. 8). Extrinsic defects may also be present in the coating layers beyond the first few near the substrate surface, particularly at their interfaces due to microstructural differences between the high and low index thin films. A study[19] has, however, shown evidence that interfaces between

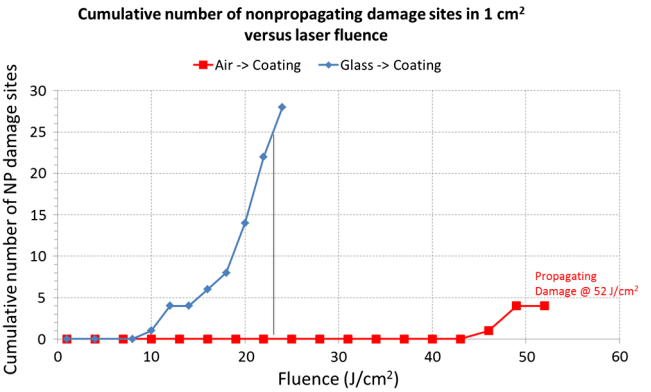

Fig. 9 Laser damage data for the dichroic beam combiner coating at 1064 nm and 22.5-deg AOI in air, Spol, and incidence on the coating from air (air → coating) and from glass (glass → coating). Lines connecting the data points are guides for the eye. The $1/e^2$ transverse beam diameters were 1.07 mm and 1.03 mm for the air → coating and glass → coating LIDT tests, respectively. See text for explanation of NP and propagating damage.

HfO_2 and SiO_2 layers deposited by e-beam evaporation provide only a small contribution to absorption at 355 nm, and to laser-induced damage by ns pulses at 351 nm. This leads us to conclude that extrinsic defects in the interfaces of the outer layers of our coating are probably minimal and of minor consequence to the NP damage behavior we observe for glass → coating incidence even though the high intensity 532 nm pulses propagate through the entire coating.

It is interesting that the 527 nm glass → coating intensity peaks for Spol, at levels of ~128% and ~104% in, respectively, the outermost and next-to-outermost HfO_2 layers [Fig. 6(b)], are stronger than their ~82% and ~67% counterparts for incidence from air [Fig. 6(a)]. Since the ~82% peak in the outermost HfO_2 layer is likely responsible for the propagating damage occurring at 7 J/cm^2 for air → coating incidence (see Fig. 8 and the discussion above), we might expect propagating damage to occur for glass → coating incidence at fluences less than 7 J/cm^2 because of the stronger intensity peaks in the two outer HfO_2 layers in that case. The LIDT results of Fig. 8 show, however, that such propagating damage is not evident at fluences up to 5 J/cm^2, and that the precipitous onset of NP damage for incidence from air satisfies the LIDT criteria of 25 or more NP damage sites at fluences between 3 and 5 J/cm^2.

Figure 9 shows the cumulative number of NP damage sites as a function of fluence from the Spol LIDT tests at 1064 nm. These results behave in a somewhat similar way to those at 532 nm in that there is a sharp contrast between LIDT behaviors for air → coating and glass → coating incidence, with the LIDT governed by propagating damage in the former case and by NP damage in the latter case. However, the propagating damage at 1064 nm (Fig. 9) occurs at a much higher fluence, 52 J/cm^2, than at 532 nm (Fig. 8). This propagating damage, as we have discussed above, could result from extrinsic or intrinsic damage mechanisms, or some combination of both. In any case, damage mechanisms that are effectively driven by the lower energy, 1064 nm photons tend to require more of them, and hence higher fluences, to reach damage thresholds. As fluences for air → coating incidence approach the 52-J/cm^2 threshold for propagating damage, they start producing a few NP damage sites (Fig. 9) related to extrinsic defects. This laser damage behavior for

air → coating incidence at 1064 nm is consistent with the E-fields [see Fig. 7(a)], which have the highest peak intensity, at ∼200% of incident intensity, in the outer SiO_2 layer and the next highest peak intensity, at ∼110% of incident intensity, in the outer HfO_2 layer near its interface with the next-to-outermost SiO_2 layer. The propagating damage as well as the minor NP damage will likely occur within either of these two outermost layers or at their interfaces. Extrinsic defects within these outer layers and at their interfaces, though sparse and of minor consequence to laser damage at near-ultraviolet wavelengths[19] as we have noted above, may be of more significant consequence to laser damage at 1054 and 1064 nm. The NP damage shown by Fig. 9 for air → coating incidence is evidence of this.

The 1064 nm, Spol LIDT results for glass → coating incidence, like their 532 nm counterparts, are characterized by a rapid rise in the cumulative number of NP damage sites as the fluence increases, in this case from 8 to 25 J/cm^2. This behavior is quite linear between 19 and 25 J/cm^2, indicating that a linear interpolation of the threshold fluence for 25 or more NP damage sites is reliable. This linear interpolation, shown by the black vertical line in Fig. 9, specifies an LIDT of ∼22 J/cm^2. The question again is why so much NP damage occurs in the glass → coating case at fluences significantly below the threshold for propagating damage in the air → coating case. A comparison of the coating layers and E-fields for the glass → coating and air → coating cases at 1054 nm provides some insight. In the former case [Fig. 7(b)], the very high intensity peak, at 400% of incident intensity, is at a depth of ∼250 nm within the Beilby layer of the optically polished substrate surface. Then the next highest intensity peak, at ∼220% of incident intensity, is in the innermost HfO_2 layer, the layer deposited directly on the optical substrate surface, and near that layer's interface with the first SiO_2 layer. That is a SiO_2-over-HfO_2 interface. This is different from the peak at ∼115% of incident intensity in the outermost HfO_2 layer in the case of air → coating incidence [Fig. 7(a)], because that peak is near the interface of the outermost HfO_2 layer with the next to outermost SiO_2 layer, which is a HfO_2-over-SiO_2 interface. In our coating process, HfO_2 and SiO_2 layers deposit at 3 and 7 Å/s, respectively. This means that there is more relaxation time in the formation of HfO_2-over-SiO_2 than SiO_2-over-HfO_2 interfaces, and this could correlate with higher microstructural stability for HfO_2-over-SiO_2 compared to SiO_2-over-HfO_2 interfaces. One study[24] found that delamination of e-beam deposited HfO_2/SiO_2 mirror coatings due to catastrophic laser damage occurs preferentially at SiO_2-over-HfO_2 interfaces, and another study[25] found similar delamination behavior for Ta_2O_5/SiO_2 narrow band-pass filter coatings. This indicates that the bonding force of SiO_2 layers to high index layers on which they are deposited is weaker than that of high index layers to SiO_2 layers on which they are deposited. The latter study[25] attributes higher defect densities to the Ta_2O_5-over-SiO_2 interfaces because the filter coating of that study exhibited initiation of laser damage at those interfaces. That conclusion may, however, be fortuitous because the E-field intensities for that filter coating peaked only at the Ta_2O_5-over-SiO_2 interfaces and were at minima of near zero intensity at the SiO_2-over-Ta_2O_5 interfaces. This means the SiO_2-over-Ta_2O_5 interfaces of that study may also have had as high or even higher defect densities which did not initiate laser damage simply because of the near zero E-field intensity at those interfaces.[25] We are, therefore, not convinced that our HfO_2-over-SiO_2 interfaces have more defects or are less microstructurally stable than our SiO_2-over-HfO_2 interfaces. Higher microstructural stability for HfO_2-over-SiO_2 interfaces correlates not only with their stronger mechanical bond[24] but also with the increase of NP damage at 1064 nm for glass → coating compared to air → coating incidence, which is what we observe (Fig. 9).

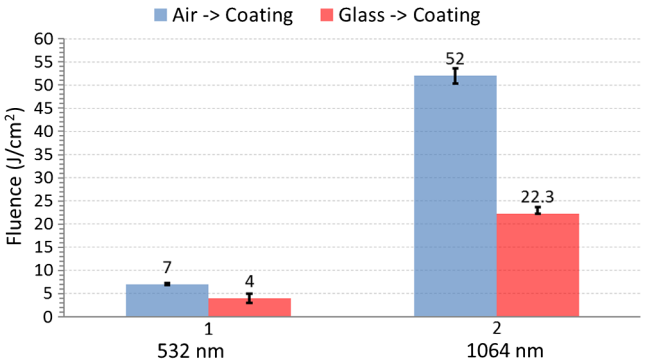

Fig. 10 LIDTs of the dichroic beam combiner coating for 22.5-deg AOI in air, Spol at 532 and 1064 nm, and incidence on the coating from air (air → coating) and from glass (glass → coating).

The other aspect of glass → coating incidence at 1054 nm is that the peak E-field intensity, at 400% of incident intensity, is in the optical substrate at a depth of ∼250 nm from the substrate/coating interface. This submicron depth is within the substrate's Beilby layer that results from the optical polishing process and contains microstructural defects and also polishing compound contamination.[14–16] This situation further favors the occurrence of defect-related NP damage for glass → coating incidence. The corresponding highest peak intensity for air → coating incidence is in air, so does not contribute to laser damage at all. This leads us to conclude that, for glass → coating incidence, the significant level of NP damage (Fig. 9) is likely associated with the two highest E-field intensity peaks [Fig. 7(b)]; namely, the peak within the extrinsic defect/contamination rich Beilby layer of the substrate, and the peak in the innermost HfO_2 layer near its interface with the innermost SiO_2 layer, which we understand to be more microstructurally unstable because it is a SiO_2-over-HfO_2 interface.

Figure 10 shows the above LIDT results, which pose a dilemma in choosing between options 1 and 2 for the dichroic beam combining optic (see Sec. 3 above). In either option, with the dichroic beam combining coating on sides 1 or 2 of the beam combining optic, one or the other of the 527 and 1054 nm high intensity beams will be incident on the dichroic coating from within the glass substrate. As the results shown in Fig. 10 demonstrate, the LIDT for whichever beam is incident on the coating from glass is significantly less than what it would be if that beam were incident on the coating from air. In our case, the choice between the two options is straightforward. Option 1, having the high intensity 527 and 1054 nm, ns pulses incident on the dichroic coating from, respectively, air at LIDT of ∼7 J/cm^2 and glass at LIDT of ∼22 J/cm^2, is better than option 2. That is because both of our high intensity beams are of comparable energies per pulse. To go with option 2

would mean operating with the higher ~52 J/cm^2 LIDT at 1054 nm but a lower, limiting LIDT of ~(4 ± 1) J/cm^2 at 527 nm. Option 1 affords the higher ~7 J/cm^2 as the limiting LIDT. It does, however, impose a lower, ~22 J/cm^2 LIDT at 1054 nm, but this is more acceptable compared to the other way around.

6 Summary and Conclusions

In summary, we have described an application for a dichroic beam combining optic for HT at 527 nm and HR at 1054 nm for 22.5-deg AOI, Spol in the context of meter scale optics and large scale, petawatt class laser systems. The requirement at 527 nm of HT makes achieving corresponding high LIDT particularly challenging because the high intensity 527 nm pulses pass at nearly full energy through all of the dichroic coating layers. We presented and explained our approach to designing the dichroic beam combiner coating using layers of near HWOT in the design space for stable HT at 527 nm, and with layer modifications that provide HR at 1054 nm while preserving HT at 527 nm. Next, we pointed out the two options for implementing the dichroic coating and beam combining optic in the laser beam train, with the coating on side 1 of the optic in option 1 and on side 2 of the optic in option 2. This raised the question of differences between air → coating incidence and glass → coating incidence of the high intensity 527 and 1054 nm, ns pulses on the dichroic coating, and led to our analysis of corresponding differences with respect to the E-field behaviors in the air and glass incident media and within the dichroic coating. That analysis indicated that, for both 527 and 1054 nm, the LIDTs for air → coating incidence should be higher than for glass → coating incidence. We next presented LIDT measurements for 532 and 1064 nm which confirmed that analysis showing that the LIDTs for glass → coating incidence are less than those for air → coating incidence by factors of ~0.6 and ~0.4 at 532 and 1064 nm, respectively. Our interpretation of the measurements centers around careful arguments explaining how the LIDT data (Figs. 8 and 9) correlates with the E-field behaviors (Figs. 6 and 7). These arguments take into account laser damage due to the intrinsic, electronic properties of the coating layers, and also due to extrinsic defects such as contamination, particulates, or nodules within the coating layers as well as the Beilby layer of the polished optic surface, and to possible differences between the microstructural stability of HfO_2-over-SiO_2 compared to SiO_2-over-HfO_2 layer interfaces. Our E-field analysis and the LIDT results support the choice of option 1 for the beam combining optic configuration, according to which the high intensity 527 and 1054 nm beams are incident on the dichroic coating from air and glass, respectively, and the limiting LIDT at 527 nm is ~7 J/cm^2 rather than ~(4 ± 1) J/cm^2 while that at 1054 nm is ~22 J/cm^2 rather than ~52 J/cm^2.

Though we developed and optimized the dichroic coating design for incidence on the coating from air, we could have explored optimal designs for incidence on the coating from glass in order to obtain E-fields more favorable to higher LIDTs for glass → coating incidence while still being favorable to high LIDTs for air → coating incidence. It would, however, not be possible to have HR at 1054 nm for glass → coating incidence without a very large, resonant E-field intensity peak, at ~400% of incident intensity, at submicron depth within the optical substrate. The NP, defect-related damage associated with that large E-field intensity peak within and near the Beilby layer of the substrate would limit the 1054-nm LIDT to fluences below that for intrinsic laser damage, just as we found for our dichroic coating. The ~7 J/cm^2 limiting LIDT at 527 nm is only marginally adequate for our dichroic beam combining applications, and this gives us motivation to look for dichroic coating designs that afford higher limiting LIDTs.

Acknowledgments

Sandia National Laboratories is a multimission laboratory managed and operated by Sandia Corporation, a wholly owned subsidiary of Lockheed Martin Corporation, for the US Department of Energy's National Nuclear Security Administration under contract DE-AC04-94AL85000.

References

1. J. C. Bellum et al., "Design and laser damage properties of a dichroic beam combiner coating for 22.5° incidence and S polarization with high transmission at 527 nm and high reflection at 1054 nm," *Proc. SPIE* **9632**, 96321E (2015).
2. Sandia Z-Backlighter Lasers, www.z-beamlet.sandia.gov (30 September 2016).
3. O. Stenzel et al., "Investigation on the reproducibility of optical constants of TiO_2, SiO_2, and Al_2O_3 films, prepared by plasma ion assisted deposition," *Opt. Mater. Express* **5**(9), 2006–2023 (2015).
4. E. Field et al., "How laser damage resistance of HfO_2/SiO_2 optical coatings is affected by embedded contamination caused by pausing the deposition process," *Proc. SPIE* **9532**, 95320J (2015).
5. R. R. Willey, "Comparative experience in the use of "steering" in automatic and manual optical monitoring," in *Proc. of the 37th Annual Technical Conf. of the Society of Vacuum Coaters*, pp. 113–117 (1994).
6. A. Dinca et al., "Dichroic mirror design by complete admittance matching," *Opt. Eng.* **35**(5), 1284–1287 (1996).
7. X. Ma et al., "Elimination of the half-wave hole for short-wave pass filter," *Proc. SPIE* **5774**, 377–380 (2004).
8. H. Jiao et al., "Study of HfO_2/SiO_2 dichroic laser mirrors with refractive index inhomogeneity," *Appl. Opt.* **53**(4), A56–A61 (2014).
9. OptiLayer Thin Film Software, www.optilayer.com (30 September 2016).
10. J. Bellum et al., "Meeting thin film design and production challenges for laser damage resistant optical coatings at the Sandia large optics coating operation," *Proc. SPIE* **7504**, 75040C (2009).
11. J. Bellum et al., "Production of optical coatings resistant to damage by petawatt class laser pulses," in *Lasers—Applications in Science and Industry*, K. Jakubczak, Ed., InTech Open Access Publisher, Rijeka, Croatia (2011).
12. J. Bellum et al., "Comparisons between laser damage and optical electric field behavior for hafnia/silica antireflection coatings," *Appl. Opt.* **50**(9), C340–C348 (2011).
13. J. Bellum et al., "Laser damage by ns and sub-ps pulses on hafnia/silica anti-reflection coatings on fused silica double-sided polished using zirconia or ceria and washed with or without an alumina wash step," *Proc. SPIE* **7842**, 784208 (2010).
14. D. Tomka et al., "Development of methodology for evaluation of subsurface damage," *Proc. SPIE* **9442**, 94421B (2015).
15. G. Hu et al., "Influence of subsurface defects on 355 nm laser damage resistance of monolayer and multilayer coatings," *Proc. SPIE* **7504**, 75040D (2009).
16. Y. Jun et al., "Surface structure of fused silica revealed by thermal annealing," *Proc. SPIE* **9238**, 92380F (2014).
17. Spica Technologies, Inc., www.spicatech.com (30 September 2016).
18. "Small optics laser damage test procedure," NIF Technical Report MEL01-013-0D, Lawrence Livermore National Laboratory, Livermore, California (2005).
19. S. Papernov et al., "Interface absorption versus film absorption in HfO_2/SiO_2 thin-film pairs in the near-ultraviolet and the relation to pulsed-laser damage," *Proc. SPIE* **9237**, 92370Q (2014).
20. X. Liu et al., "Characteristics of plasma scalds in multilayer dielectric films," *Appl. Opt.* **50**(21), 4226–4231 (2011).
21. B. Liao et al., "The formation and development of nodular defects in optical coatings," in *Damage in Laser Materials: 1985*, H. E. Bennett et al. Eds., Vol. **746**, pp. 305–318, National Bureau of Standards (US) Special Publication (1987).
22. C. J. Stolz and F. Y. Genin, "Laser resistant coatings," in *Optical Interference Coatings*, N. Kaiser and H. K. Pulker, Eds., Springer-Verlag, Berlin Heidelberg (2003).

23. W. Rudolph et al., "Laser damage in thin films: what we know and what we don't," *Proc. SPIE* **8885**, 888516 (2013).
24. X. Liu et al., "Investigations on the catastrophic damage in multilayer dielectric films," *Appl. Opt.* **52**(10), 2194–2199 (2013).
25. Z. Wang et al., "Interfacial damage in a Ta_2O_5/SiO_2 double cavity filter irradiated by 1064 nm nanosecond laser pulses," *Opt. Express* **21**(25), 30623–30632 (2013).

John C. Bellum received a BS (Georgia Institute of Technology, 1968) and a PhD (University of Florida, 1976), both in physics. He has numerous scientific publications and extensive experience as a physicist and optical engineer. He provides technical leadership for the Large Optics Coating Facility at Sandia National Laboratories (SNL), specializing in high laser damage threshold optical coatings for large, meter-size optics for petawatt class lasers. He is a senior member of both SPIE and OSA.

Ella S. Field is an engineer at SNL in Albuquerque, New Mexico, USA. She manages operations at the Optical Support Facility and develops optical coatings for the Z-Backlighter Laser. She received bachelor's degrees in mechanical engineering and Asian languages and literature from the University of Minnesota in 2009, and received a master's degree in mechanical engineering from the Massachusetts Institute of Technology in 2011.

Damon E. Kletecka is an optical coating technologist at SNL in Albuquerque, New Mexico, USA. He has spent the past 12 out of 13 years at Sandia with the Large Optics Coating Facility, supporting the general operation and maintenance of the coating system.

Patrick K. Rambo received his BA degree in applied physics from Rice University in 1993. He received his PhD in optical sciences from the University of New Mexico in 2000 for dissertation research on laser-triggered lightning. Since 2000, he has been at SNL working mostly at the Z-Backlighter facility. He was part of the teams there which activated the kilojoule-class Z-Beamlet laser for radiography and which developed the Z-Petawatt system.

Ian C. Smith received a BSc (honors) from Essex University, England, in 1985, and became a scientific officer that year for the HELEN laser at the Atomic Weapons Establishment (AWE). During 1993 to 1996, he worked with the NIF prototype laser (Beamlet) at Lawrence Livermore National Laboratory, returning to work on AWE's HELEN upgrade. In 2000, he began working with Beamlet (renamed Z-Beamlet) at SNL, and joined SNL in 2002 to oversee Z-Beamlet operations.